RSC Advances

PAPER

View Article Online
View Journal | View Issue

Cite this: *RSC Adv.*, 2024, **14**, 13452

An efficient catalysis for the synthesis of pyrimido [1,2-*a*]benzimidazoles and 1-(benzothiazolylamino) methyl-2-naphthols using ZnO@SO_3H@Tropine†

Fatemeh Rahimizadeh, Masoumeh Mazloumi and Farhad Shirini *

Received 31st December 2023
Accepted 30th March 2024

DOI: 10.1039/d3ra08960f

rsc.li/rsc-advances

In this research and in the line of our researches on the use of nano-substrates modified with ionic liquid in organic reactions, an efficient and green method for the one-pot three-component synthesis of pyrimido [1,2-*a*]benzimidazole and 1-(benzothiazolylamino)methyl-2-naphthol derivatives is reported using a new nanoporous catalyst formulated as ZnO@SO_3H@Tropine. Further analysis of the catalyst for its characterization has been performed using thermal gravimetric analysis (TGA), field emission scanning electron microscopy (FESEM), X-ray diffraction (XRD), energy dispersive spectrometer (EDS) and Fourier-transform infrared spectroscopy (FT-IR). The present approach creates a variety of biologically active heterocyclic compounds with excellent yields and short reaction times. Among the other advantages of the current method are: ease of operation, clean reaction profiles and ease of separation. Also, this catalyst can be reused five times without loss of its catalytic activity.

Introduction

As a part of green chemistry and because of global environmental concerns, it is important to use catalysts, avoid using hazardous chemical solvents and reduce waste materials in organic reactions. The multi-component reactions (MCRs) are powerful tools used in the synthesis of some chemical compounds.[1] The use of MCRs under solvent-free conditions has attracted considerable interest from chemists, especially from the standpoint of green chemistry.[2] There are many advantages for using these methods, such as waste reduction, operational ease, mild reaction conditions, selectivity and high efficiency.[3]

Nitrogen-containing heterocyclic compounds are an important class of organic compounds with a special place among natural products and pharmaceutical compounds.[4,5] The nitrogen atoms in heterocyclic structures are pivotal in determining the compounds' biological activity because allowing for crucial interactions with biological macromolecules such as proteins and enzymes, and ultimately determine their overall effectiveness in biological systems. Among the natural compounds containing nitrogen include pyridine derivatives, such as natural pyridine alkaloid trichodin A, sulfapyridine, and natural spiroindoles isolated from plants and microorganisms the whole plant of *Flueggea virosa*.[6–10]

Department of Chemistry, College of Science, University of Guilan, Rasht, 41335-19141, Iran. E-mail: shirini@guilan.ac.ir; fshirini@gmail.com; Fax: +98 131 3233262; Tel: +98 131 3233262

† Electronic supplementary information (ESI) available. See DOI: https://doi.org/10.1039/d3ra08960f

An important class of these compounds are benzimidazole and benzothiazole derivatives which exhibit a range of biological properties such as antimicrobial,[11] antibacterial,[12] anti-tumor,[13] anticancer,[14] anti-fungal[15] and anti-inflammatory.[16] Also, they are known in drugs designed to target DNA and DNA-related processes.[17] Additionally, some natural bioactive compounds like vitamin B12 (ref. 1) and vitamin B1 (ref. 18) contain the benzimidazole nucleus.

Nowadays, synthesis of pyrimido[1,2-*a*]benzimidazole and 1-(benzothiazolyl amino)methyl-2-naphthol derivatives, has attracted the attention of organic chemistry researchers and for the synthesis of them, a variety of catalysts have been employed some of these catalysts are $[(CH_2)_3SO_3HMIM]HSO_4$,[19] sodium dodecyl sulfate (SDS),[20] trichloroisocyanuric acid (TCCA),[21] phosphate fertilizers,[22] MgO,[23] nano ZnO,[24], [bmim][BF_4],[25] *S*-Chit-HAp@Fe_3O_4,[26] $ZnClO_4$ (ref. 27) and nano-sawdust-OSO_3H.[28] Although these methods have their advantages, most of them are accompanied with disadvantages, such as hazardous solvent, long reaction times, high temperature reactions, low yields, high costs, and need to use of large amounts of catalysts.[29]

Zinc oxide is used in more than a hundred different fields, ranging from large-scale products to more advanced applications.[30] As well as in many different industrial sectors, including photocatalysis, pigments, rubber, ceramics, food and cream additives.[31] Also, because that ZnO nanoparticles are able to absorb UV light, they are used as sunscreens, and due their antibacterial properties, they can be used as pastes and plasters to treat wounds.[30]

In recent decades, because they complied with the principles of green chemistry, nanomaterials have appeared as important

heterogeneous reagents for the acceleration of catalytic processes. There are many benefits of using zinc oxide nanostructures as an efficient nanocatalysts, such as cost effectiveness, non-toxicity, environmentally friendly, and large surface area. These nanostructures are widely used for various organic transformations such as the Mannich and Knoevenagel condensation reactions.[32]

Furthermore, because of their low vapor pressure, thermal and chemical stability, ease of handling, environmental friendliness, and the ability to dissolve most organic and inorganic substances, ionic liquids (ILs) are used as catalyst and solvent.[33] In spite of the mentioned advantages high cost, large consumption, and difficult recovery are limitations for their use at large scale. Additionally, ionic liquids (particularly Brønsted acidic ionic liquids) are unstable in the presence of air and moisture.

Ionic liquid immobilization on solid supports is an effective method for combining the advantages of ionic liquids with solid properties. Basically, immobilized ionic liquids offer a number of advantages over pure ionic liquids that facilitate their handling, separation, and reuse procedures, and minimize the amounts of the used ILs.[34]

In this study, we synthesized a new catalyst using the reaction of tropine with sulfonic acid functionalized nano-porous ZnO (ZnO@SO_3H@Tropine). Introduced catalyst was used for the promotion of the synthesis of pyrimido[1,2-*a*]benzimidazole and 1-(benzothiazolylamino)methyl-2-naphthol derivatives. As a result, this process provides short reaction times and high yields (95–99%). In addition, the catalyst can be easily removed and used at least for five times without sacrificing much efficiency.

Experimental

Chemicals were purchased from Fluka, Sigma-Aldrich and Merck Chemical Companies. And used without further purification. The products were identified by comparing their melting points and spectral data with those reported in the literature. Yields refer to the isolated products.

Preparation of ZnO@SO_3H@Tropine

A suspension of ZnO (1 g) was prepared in 20 mL of dry CH_2Cl_2. Then, with vigorous stirring, concentrated $ClSO_3H$ (0.5 mL) was added dropwise to it in an ice bath (0 °C). The mixture was warmed to room temperature, and stirred for 24 hours. A gas outlet tube was also used to conduct HCl gas into water as an absorbing solution. ZnO@SO_3H as a white powder is obtained by washing with diethyl ether (2 × 10 mL), filtration, and drying at 70 °C. In the next step, tropine (3 mmol) was added to a mixture of ZnO@SO_3H in CH_3CN (20 mL). The reaction mixture was refluxed with stirring for 2 days. Finally, the product was washed with diethyl ether (2 × 10 mL) and dried at 70 °C to afford ZnO@SO_3H@Tropine as the product (Scheme 1).

General procedure for the synthesis of pyrimido[1,2-*a*] benzimidazole derivatives

A mixture of aldehyde (1 mmol), 2-aminobenzimidazole (1 mmol), malononitrile (1.2 mmol) and ZnO@SO_3H@Tropine (30 mg) was heated under solvent-free conditions at 120 °C for the appropriate time. After completion of the reaction which was identified by TLC [*n*-hexane : ethyl acetate (7 : 3)], EtOH was added and the catalyst was separated by filtration and the precipitated product was separated by evaporation of EtOH in high purity.

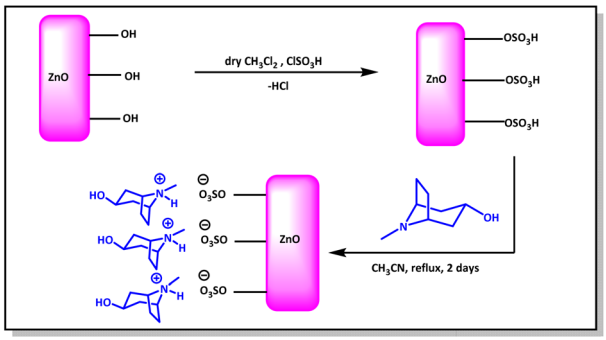

Scheme 1 Preparation of the nano-porous ZnO@SO_3H@Tropine.

The spectral data of a compound is as follows: 2-amino-4-(4-bromophenyl)-1,4-dihydrobenzo[4,5]imidazo[1,2-*a*] pyrimidine-3-carbonitrile (**3a**) white solid; Mp: >300 °C yield; 95%; ^{1}H NMR (400 MHz, DMSO-d_6): δ = 5.24 (s, 1H, –CH aliphatic), 6.87 (brs, 2H), 7.01 (t, 1H, J = 8 Hz), 7.12 (t, 1H, J = 8 Hz), 7.24 (t, 3H, J = 8 Hz), 7.56 (d, 2H, J = 8 Hz), 7.62 (d, 1H, J = 8 Hz), 8.60 (brs, 1H) ppm; ^{13}C NMR (100 MHz, DMSO-d_6): δ = 52.5, 61.3, 112.4, 116.1, 119.0, 119.9, 120.9, 123.3, 128.2, 129.2, 131.5, 142.1, 143.5, 149.2, 151.5 ppm.

General procedure for the synthesis of 1-(benzothiazolylamino)methyl-2-naphthol derivatives

A mixture of 2-aminobenzothiazole (1 mmol), β-naphthol (1 mmol), aldehyde (1 mmol) and ZnO@SO_3H@Tropine (10 mg) was heated in an oil bath at 120 °C for an appropriate time. After completion of the reaction (monitored by TLC [*n*-hexane : ethyl acetate (7 : 3)]), EtOH was added and the catalyst was separated by filtration and the precipitated product was separated by evaporation of EtOH in high purity.

The spectral data of a compound is as follows: 1-((benzo[*d*] thiazol-2-ylamino)(3-nitro-phenyl)methyl)naphthalen-2-ol (**7b**): Mp: 198–200 °C; yield; 90%; ^{1}H NMR (400 MHz, DMSO-d_6) 8.31 (s, 1H), 8.05–7.99 (d, 1H, J = 9.2 Hz), 7.99 (s, 1H), 7.77 (d, 1H, J = 8.0 Hz), 7.72 (d, 1H, J = 8.9 Hz), 7.67 (d, 1H, J = 7.7 Hz), 7.54 (d, 1H, J = 7.8 Hz), 7.50 (d, 1H, J = 8.0 Hz), 7.46–7.41 (m, 1H), 7.38 (t, 1H, J = 8.0 Hz), 7.30–7.22 (m, 4H), 7.05 (t, 1H, J = 7.6 Hz). ^{13}C NMR (100 MHz, DMSO-d_6) 166.58, 153.80, 152.37, 148.21, 145.84, 133.33, 132.41, 131.38, 130.66, 130.18, 129.19, 128.99, 127.22, 125.95, 123.62, 123.11, 121.83, 121.72, 121.46, 120.93, 118.83, 118.17, 53.16 ppm.

Results and discussion

Instrumentations

Substrate purity determination and reaction control were done by TLC on silica gel polygram SILG/UV254 plates. Electro-

thermal melting point apparatus IA9100 was used to determine melting points in capillary tubes. The Fourier-transform infrared spectra (FT-IR) were recorded with a VERTEX 70 (Brucker, Germany) instrument using KBr pellets for the obtained solid samples. X-ray diffraction (XRD) was performed on an X'Pert Pro instrument (Panalytical Company Netherlands). Field emission scanning electron microscopy (FESEM) was recorded using a TE-SCAN model Sigma VP (ZEISS Company in Germany). Thermogravimetric analysis (TGA) was performed on a TGA-DTA METTLER TGA/STTA 851 (Swiss). Energy dispersive spectrometer (EDS) was performed on a TESCAN model MIRA III (France).

Characterization of the catalyst

Energy dispersive spectrometer (EDS). The EDS results of ZnO@SO_3H@Tropine indicate the presence of all expected elements (C, O, N, S, and Zn) (Fig. 1). The existence of C, N and S elements demonstrates the successful immobilizing of ionic liquid on ZnO.

Fig. 2 compares the FT-IR spectra of ZnO, ZnO@SO_3H and ZnO@SO_3H@Tropine. In the FT-IR spectrum of ZnO, the absorption bands at 3410 and 1592 cm^{-1} are related to the stretching and bending vibrations the hydroxyl group.[34] In addition, the peaks at 874 and 563 cm^{-1} are corresponded to the stretching vibrations of Zn–OH and Zn–O bands, respectively.[35] In the FT-IR spectrum of ZnO@SO_3H, asymmetric and symmetric stretching modes of O═S═O and stretching mode of S–O bands of sulfonic groups are appeared at 1111, 1019, and 620 cm^{-1}, respectively.[36] In the FT-IR spectrum of ZnO@SO_3-H@Tropine, absorption bands at 2500–3000 cm^{-1} and 1041 cm^{-1} are related to the C–H and C–N stretching vibrations of tropine, which indicates that the ionic liquid moiety was formed on the substrate surface.[37]

The thermogravimetric analysis (TGA) of ZnO and ZnO@SO_3H@Tropine is presented in order to compare the thermal stability of them (Fig. 3). As the curves show, ZnO have high thermal stability and slight weight loss (about 4%) on the curve of this reagent is related to the loss of the physically adsorbed water and terminal groups such as –OH ones.[38] The

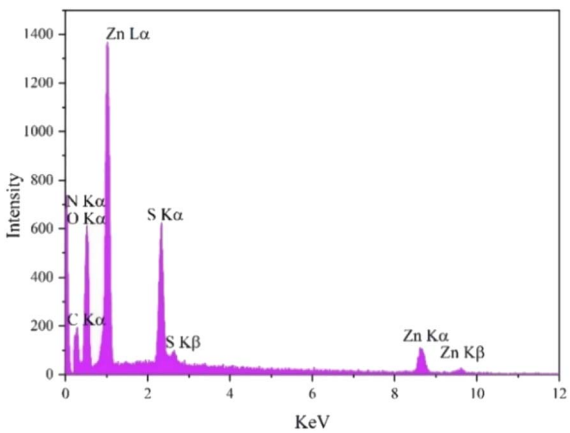

Fig. 1 The EDS profiles of ZnO@SO_3H@Tropine.

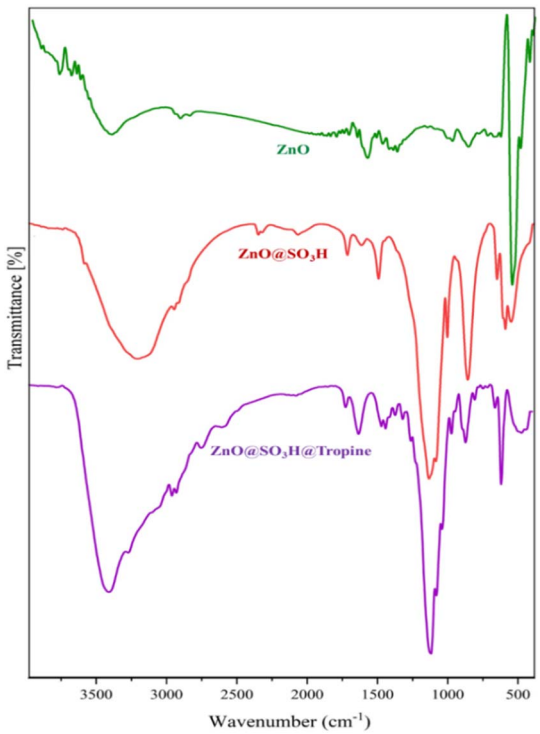

Fig. 2 FT-IR spectra of ZnO, ZnO@SO_3H and ZnO@SO_3H@Tropine.

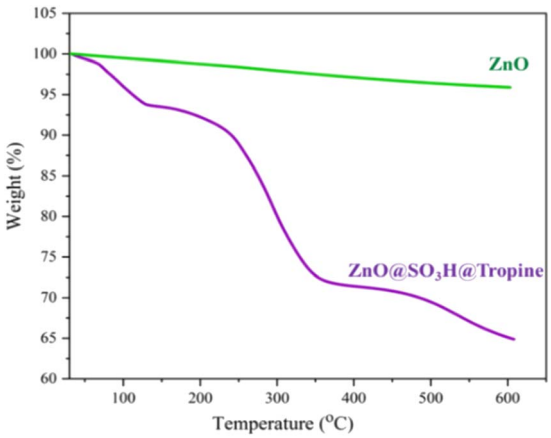

Fig. 3 TGA curve of ZnO and ZnO@SO_3H@Tropin.

TGA curve of ZnO@SO_3H@Tropine is completely different from ZnO. In this curve the lost weight below 120 °C can be ascribed to the removal of the adsorbed water and the two weight losses at about 250 and 500 °C can be related to the decomposition of the sulfonic groups and the organic part in the ionic liquid on the surface of the support.

X-ray diffraction (XRD) analysis of ZnO and ZnO@SO_3-H@Tropine are shown in Fig. 4. In the XRD pattern of ZnO, eleven peaks are appeared at around 2θ = 31.8, 34.5, 36.25, 47.65, 56.65, 62.95, 66.4, 68.00, 69.15, 72.55 and 77.05 that are corresponded to the (100), (002), (101), (102), (110), (103), (200), (112), (201), (004) and (202) planes of ZnO.[39] In the XRD pattern of ZnO@SO_3H@Tropine, in addition to the mentioned peaks,

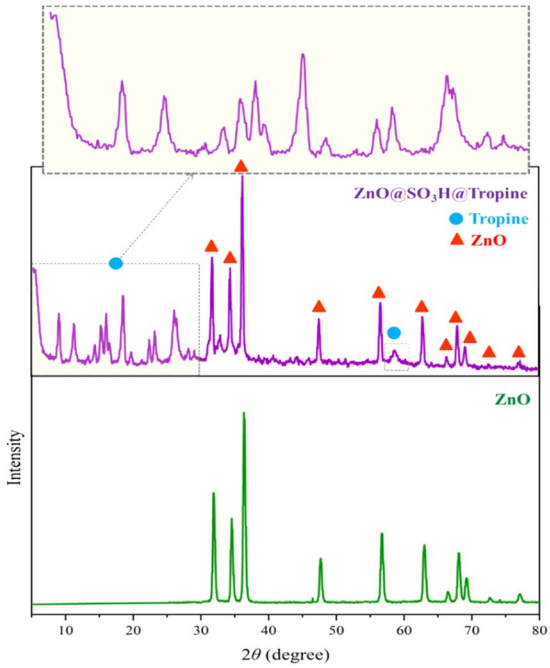

Fig. 4 XRD patterns of ZnO and ZnO@SO_3H@Tropine.

various peaks were appeared which are indicated the presence of the ionic liquid on ZnO by maintaining the main structure of the support.

Field emission scanning electron microscopy (FESEM). The field emission scanning electron microscopy (FESEM) images of ZnO and ZnO@SO_3H@Tropine specifies the surface morphology, size distribution and particle shape of them (Fig. 5). Comparison of the pictures show that in the catalyst, the particles of the support are aggregated after modification with the ionic liquid which can be a result of the hydrogen bonding and also dipole–dipole attraction between the ionic liquids moieties.

Catalytic activity

Based on the information obtained from the structural studies on ZnO@SO_3H@Tropine, we predicted that this reagent could be used as a solid acid catalyst to accelerate reactions that require an acidic catalyst for the acceleration. As a result, we were interested in exploring the potential of this reagent in promoting the synthesis of pyrimido[1,2-*a*]benzimidazole and 1-(benzothiazolylamino)-phenylmethyl-2-naphthols.

For this purpose, two model reactions (the synthesis of 2-amino-4-(4-chlorophenyl)-1,4 dihydrobenzo[4,5]imidazo[1,2-*a*]

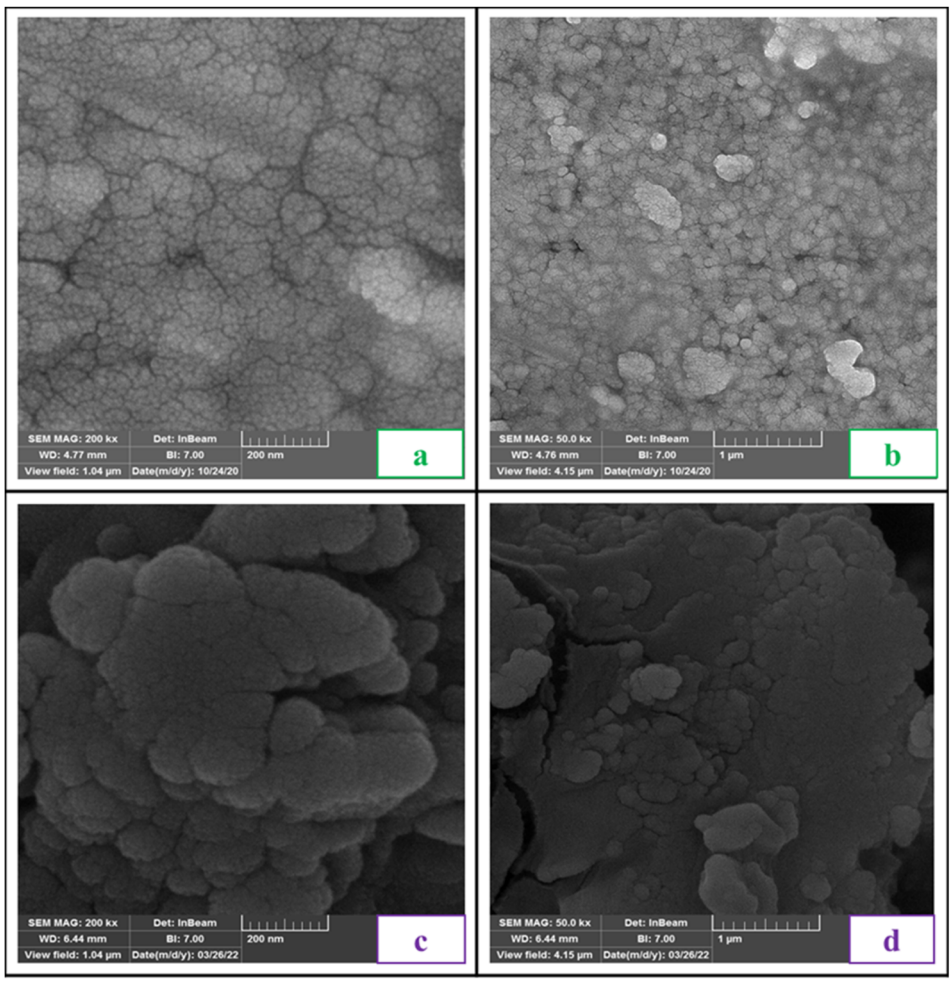

Fig. 5 FESEM images of ZnO (a and b) and ZnO@SO_3H@Tropine (c and d).

pyrimidine-3-carbonitrile and 1-((benzo[*d*]thiazol-2-ylamino)(2,4-dichlorophenyl)methyl)naphthalen-2-ol) were selected and their conditions were optimized under the influence of various conditions, such as different amounts of the ZnO@SO_3H@Tropine catalyst, presence and absence of solvent and different temperatures. The results are outlined in Table 1.

The obtained results show that performing the reaction under solvent-free conditions at the 120 °C is suitable for the completion of the studied reactions in shorter reaction times. In addition, the best results can be obtained in the presence of 30 and 10 mg of the catalyst for the synthesis of the compounds **1a** and **6b**, respectively (Table 1, entries 5 and 15) (Scheme 2).

On the other hand, absence of the catalyst caused only a trace amounts of the products to be obtained for both reactions. In continue the generality of this method was studied by using various types of aromatic aldehydes for the synthesis of their corresponding pyrimido[1,2-*a*]benzimidazole and 1-(benzothiazolylamino)methyl-2-naphthol derivatives under the optimal conditions. Based on the data reported in Table 2, under the selected conditions, a wide range of aldehydes with both electron-donating and electron-withdrawing substituents

Table 1 Optimizations of the reaction conditions in the synthesis of 2-amino-4-(4-chlorophenyl)-1,4-dihydrobenzo[4,5]imidazo[1,2-*a*]pyrimidine-3-carbonitrile and 1-((benzo[*d*]thiazol-2-ylamino)(2,4-dichlorophenyl)methyl)naphthalen-2-ol

Entry	Product	Catalyst (mg)	Solvent	Temperature (°C)	Time (min)	Conversion (%)
1		30	Solvent-free	100	13	100
2		20	Solvent-free	100	17	100
3		10	Solvent-free	100	22	100
4		40	Solvent-free	100	22	100
5	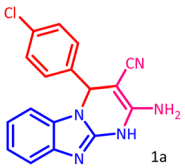 1a	**30**	**Solvent-free**	**120**	**4**	**100**
6		30	Solvent-free	80	40	—[a]
7		30	CH_3CN	80	40	—[a]
8		30	EtOH	75	70	Trace
9		30	H_2O	90	60	—[a]
10		—	No solvent	120	100	Trace
11		20	Solvent-free	100	75	—[a]
12		10	Solvent-free	100	40	—[a]
13		5	Solvent-free	100	60	—[a]
14		30	Solvent-free	100	100	Trace
15	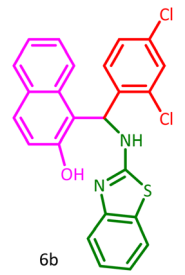 6b	**10**	**Solvent-free**	**120**	**15**	**100**
16		20	Solvent-free	120	60	—[a]
17		5	Solvent-free	120	50	—[a]
18		10	Solvent-free	80	80	—[a]
19		40	EtOH	70	130	Trace
20		40	Water	90	150	Trace
21		40	EtOH/H_2O (1 : 1)	75	145	Trace
22		—	Solvent-free	120	160	Trace

[a] The reaction was not completed.

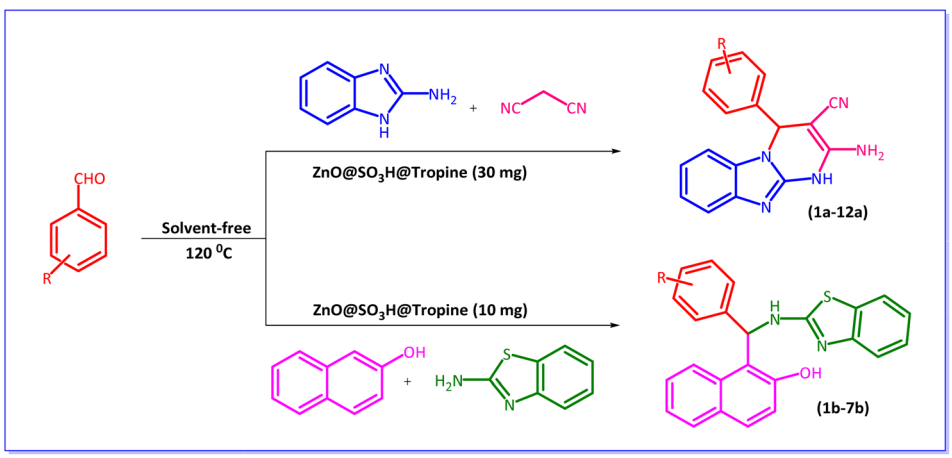

Scheme 2 One-pot three-component synthesis of pyrimido[1,2-*a*]benzimidazole and 1-(benzothiazolylamino)methyl-2-naphthol derivatives catalyzed by ZnO@SO_3H@Tropine.

Table 2 Synthesis of pyrimido[1,2-*a*]benzimidazole and 1-(benzothiazolylamino)methyl-2-naphthol derivatives using ZnO@SO_3H@Tropine

Entry	Aldehyde	Product	Time (min)	Yield[a] (%)	MP (°C) Found	MP (°C) Reported (ref.)
1		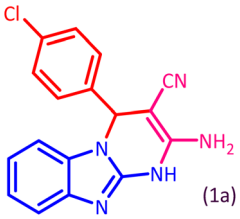 (1a)	4	99	234–236	235–237 (ref. 40)
2		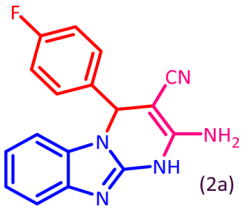 (2a)	3	98	230–231	232 (ref. 41)
3		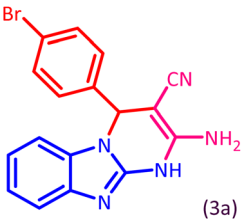 (3a)	14	95	>300	307–309 (ref. 42)
4	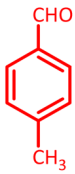	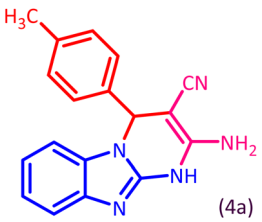 (4a)	12	95	219–222	222–225 (ref. 29)
5	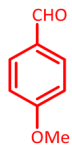	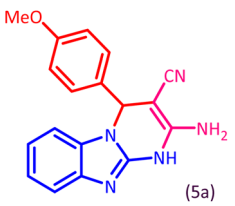 (5a)	5	97	229–230	232–234 (ref. 43)
6	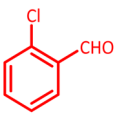	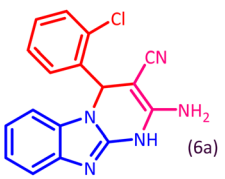 (6a)	10	95	234–235	236–238 (ref. 40)
7	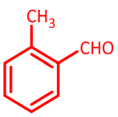	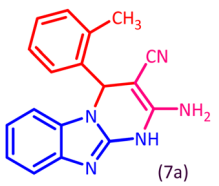 (7a)	3	96	232–233	233–235 (ref. 2)

Table 2 (*Contd.*)

Entry	Aldehyde	Product	Time (min)	Yield[a] (%)	MP (°C) Found	MP (°C) Reported (ref.)
8	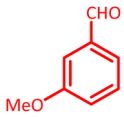	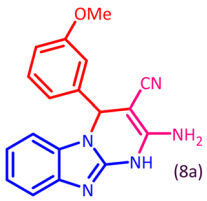 (8a)	25	92	223–225	226–244 (ref. 41)
9	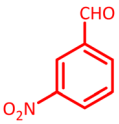	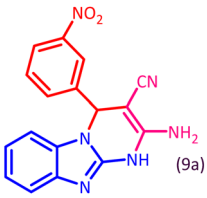 (9a)	40	85	230–232	237–239 (ref. 44)
10	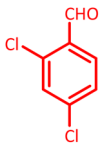	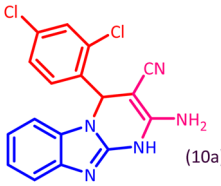 (10a)	11	94	237–238	236–239 (ref. 29)
11	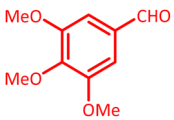	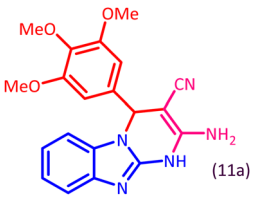 (11a)	28	91	229–230	230–232 (ref. 2)
12	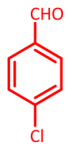	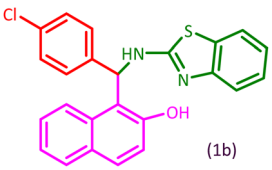 (1b)	25	98	209–211	209–211 (ref. 45)
13	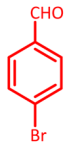	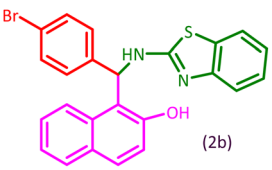 (2b)	10	98	214–216	211–213 (ref. 46)
14	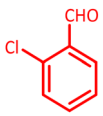	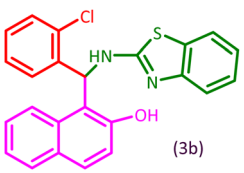 (3b)	100	90	204–206	199–200 (ref. 45)
15	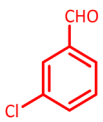	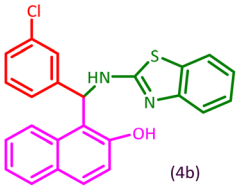 (4b)	105	80	192–194	193–194 (ref. 3)

Table 2 (*Contd.*)

Entry	Aldehyde	Product	Time (min)	Yield[a] (%)	MP (°C) Found	MP (°C) Reported (ref.)
16	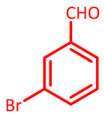	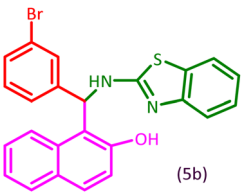 (5b)	50	85	206–208	205–206 (ref. 47)
17	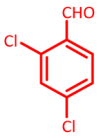	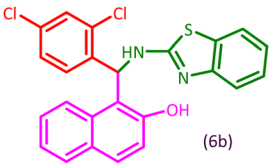 (6b)	15	98	199–200	204–206 (ref. 48)
18	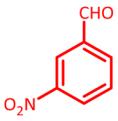	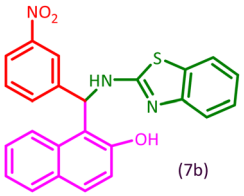 (7b)	30	90	198–200	200 (ref. 49)

[a] Isolated yields.

are converted to the corresponding products at appropriate times with excellent yields.

The comparison of the results of this study with the results reported by other catalysts in the literature was done in order to confirm the effectiveness of nanoporous ZnO@SO_3H@Tropine (Table 3). As it is shown, this method avoids several of the problems associated with other procedures, including low yields, high catalyst loading, difficult conditions for preparation of the catalyst, and long reactions times. The plausible mechanisms for the synthesis pyrimido[1,2-*a*]benzimidazole and 1-(benzothiazolylamino)methyl-2-naphthol in the presence of ZnO@SO_3H@Tropine are shown in Scheme 3. ZnO@SO_3H@Tropine as an acidic catalyst plays a significant role in activating aromatic aldehydes. According to these mechanisms,

Table 3 Comparison of the synthesis of the selected compounds using the reported methods by the present method

Product	Catalyst (mg) [ref.]	Reaction conditions	Time (min)	Yield[a] (%)
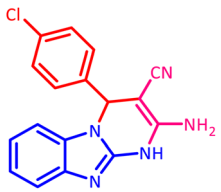	None[50]	H_2O/70 °C	720	85
	Fe_3O_4@IM (20)[43]	EtOH/reflux	15	95
	MMT-$HClO_4$ (30)[51]	Solvent-free/100 °C	25	91
	ZnO@SO_3H@Tropine (29) [This work]	Solvent-free/120 °C	4	99
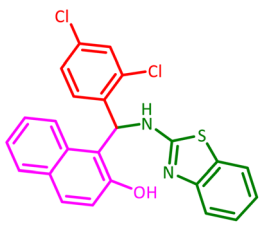	Fe_3O_4@MCM41@$ZrCl_2$ (50)[46]	Solvent-free/100 °C	15	90
	[bmim]Br (300)[52]	Solvent-free/120 °C	30	93
	Ionic liquid-functionalized SBA-15 (20)[53]	Solvent-free/120 °C	15	81
	[H-Suc]HSO_4 (30)[54]	Solvent-free/80 °C	6	93
	ZnO@SO_3H@Tropine (10) [This work]	Solvent-free/120 °C	15	98

[a] Isolated yield.

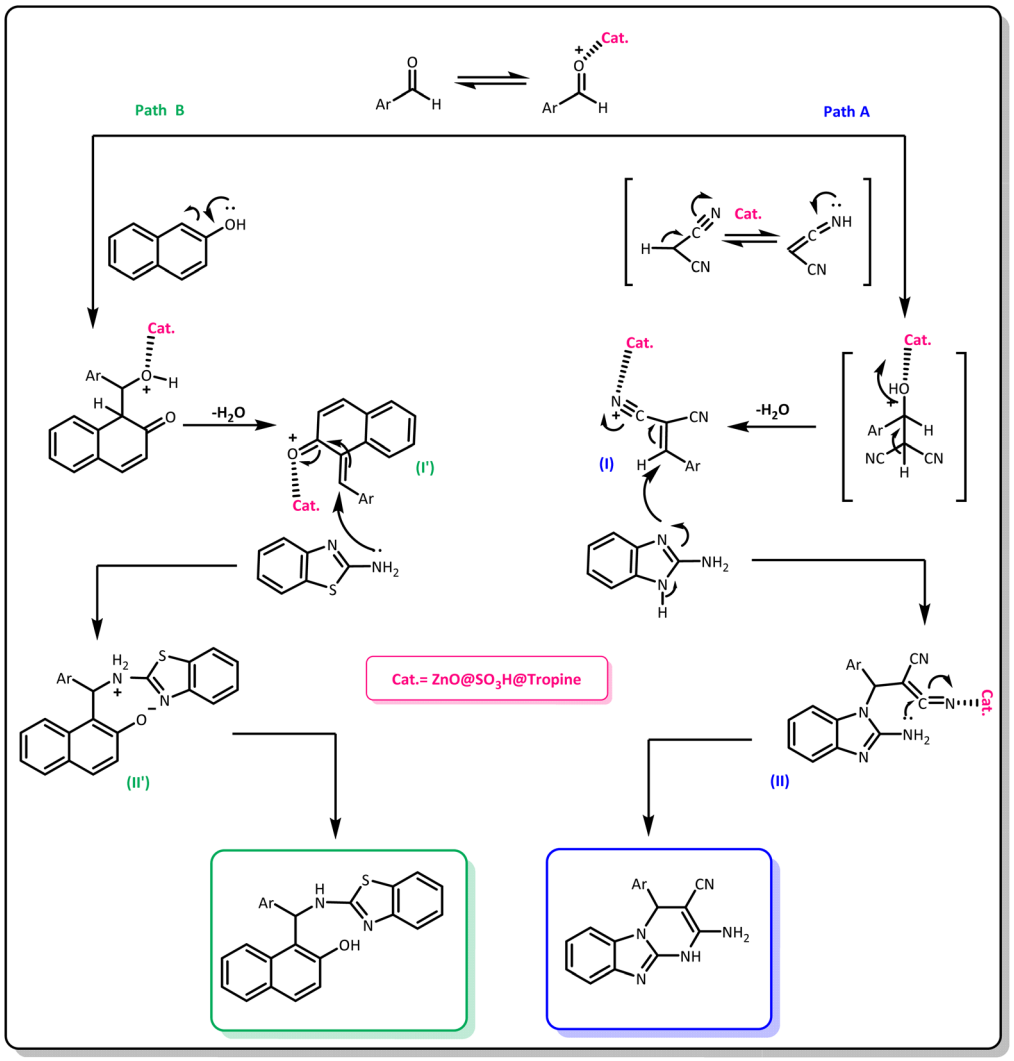

Scheme 3 The plausible mechanisms for the synthesis of 2-amino-4-phenyl-1,4-dihydropyrimido[1,2-*a*]benzimidazole-3 carbonitrile and 1-(benzothiazolylamino)methyl-2-naphthol derivatives catalyzed by ZnO@SO_3H@Tropine.

in path A, a reaction between activated aldehyde with malononitrile produces the 2-arylidenemalononitrile intermediate (**I**) by Knoevenagel condensation. In the next step, Michael addition is carried out by adding the ring nitrogen atom of 2-aminobenzimidazole to arylidenitrile (**I**). Afterwards and by intermolecular cyclization (**II**), the final product is obtained. In path B, activated aldehyde reacts with β-naphthol to form the intermediate (**I′**) that undergoes an elimination reaction to provide the intermediate (**II′**). Then, the intermediate (**II′**) is attacked by 2-aminobenzothiazole to produce the requested 1-(benzothiazolylamino)methyl-2-naphthol.

The reusability of the catalyst was also tested. To accomplish this, the reaction of 4-chlorobenzaldehyde, 2-aminobenzimidazole, and malononitrile under the optimal reaction conditions was studied again, and the catalyst was separated after the reaction was completed. The obtained catalyst was washed with ethanol, dried, and reused for the next run. Over five runs, the reaction time and yields did not significantly

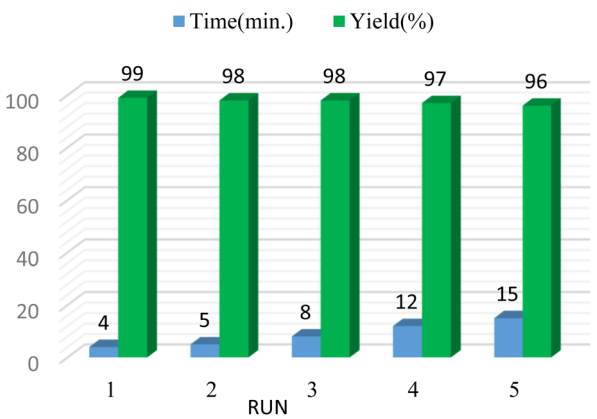

Fig. 6 Recycling of the catalyst in the synthesis of 2-amino-4-(4-chlorophenyl)-1,4-dihydrobenzo[4,5]imidazo[1,2-*a*]pyrimidine-3-carbonitrile.

change in each run. Recyclability of this catalyst was clearly demonstrated in Fig. 6.

Conclusions

In the present study, ZnO@SO_3H@Tropine was employed as a novel acidic ionic liquid catalyst immobilized on nano ZnO in the promotion of the multicomponent synthesis of pyrimido [1,2-*a*]benzimidazoles and 1-(benzothiazolylamino)methyl-2-naphthols. A significant advantage of this catalyst is its simple synthesize it from inexpensive and readily accessible materials. As well, the protocols presented here offer many benefits, including the exclusion of toxic solvents, simple work-up, excellent yields and recyclability of the catalyst. Additionally, the results indicate that this method is capable of tolerate a wide range of substituted aldehydes containing either electron-withdrawing or electron-donating groups. According to the obtained results, in addition to the preparation of new catalysts based on nano-substrates, we plan to use the introduced catalyst in the preparation of other organic compounds.

Conflicts of interest

There are no conflicts to declare.

Acknowledgements

We are thankful to the Research Council of the University of Guilan for its help to do this research.

References

1 N. Nabinia, F. Shirini, H. Tajik, M. Mashhadinezhad and M. S. N. Langarudi, *J. Iran. Chem. Soc.*, 2018, **15**, 2147.
2 M. V. Reddy, J. Oh and Y. T. Jeong, *C. R. Chim.*, 2014, **17**, 484.
3 F. Kamali and F. Shirini, *Appl. Organomet. Chem.*, 2018, **32**, 3972.
4 S. E. Mirmoeeni, M. Liyaghati-Delshad and A. Abdolmaleki, *Monatsh. Chem.*, 2020, **151**, 1135.
5 H. Nezhadramezan-Ghasemabadi, M. Mazloumi, S. K. Azimi and F. Shirini, *J. Mol. Struct.*, 2023, **1274**, 134435.
6 D. Teng, H. Zhang and A. Mendonca, *Molecules*, 2006, **11**, 700.
7 A. J. Boddy and J. A. Bull, *Org. Chem. Front.*, 2021, **8**, 1026.
8 M. Ishikura, T. Abe, T. Choshi and S. Hibino, *Nat. Prod. Rep.*, 2013, **30**, 694.
9 M. Ishikura, T. Abe, T. Choshi and S. Hibino, *Nat. Prod. Rep.*, 2015, **32**, 1389.
10 S. S. Panda, A. S. Girgis, M. N. Aziz and M. S. Bekheit, *Molecules*, 2023, **28**, 618.
11 H. Hussain, S. Aziz, B. Schulz and K. Krohn, *Nat. Prod. Commun.*, 2011, **6**, 841.
12 V. Karande, P. Mohire, P. Patil, A. Patravale, T. Bhosale, D. Chandam, D. Kumbhar and M. Deshmukh, *Res. J. Life Sci., Bioinf., Pharm. Chem. Sci.*, 2020, **6**, 134.
13 D. Heber, C. Heers and U. Ravens, *Die Pharmazie*, 1993, **48**, 537.
14 D. Kumar, P. Sharma, H. Singh, K. Nepali, G. K. Gupta, S. K. Jain and F. Ntie-Kang, *RSC Adv.*, 2017, **7**, 369770.
15 T. Singh, V. K. Srivastava, K. K. Saxena, S. L. Goel, A. Kumar and A. der Pharmazie, *J. Pharm. Anal. Med. Chem.*, 2006, **339**, 466.
16 M. T. Maghsoodlou, M. Karima, M. Lashkari, B. Adrom and J. Aboonajmi, *J. Iran. Chem. Soc.*, 2017, **14**, 329.
17 S. Bhattacharya and P. Chaudhuri, *Curr. Med. Chem.*, 2008, **15**, 1762.
18 Z. Benzekri, S. Sibous, H. Serrar, A. Ouasri, S. Boukhris, R. Ghailane, A. Rhandour and A. Souizi, *J. Mol. Struct.*, 2020, **1202**, 127308.
19 H. R. Shaterian and A. Hosseinian, *Res. Chem. Intermed.*, 2015, **41**, 793.
20 A. Kumar, M. S. Rao and V. K. Rao, *Aust. J. Chem.*, 2010, **63**, 1538.
21 L. Yang, *E-J. Chem.*, 2012, **9**, 2424.
22 O. Zimou, B. Malek, A. Elhallaoui, T. Ghailane, R. Ghailane, S. Boukhris, N. Habbadi, A. Hassikou and A. Souizi, *Bull. Chem. React. Eng. Catal.*, 2019, **14**, 238.
23 H. Sheibani and M. Babaie, *Russ. Chem. Bull.*, 2013, **62**, 2202.
24 S. Paul, P. Bhattacharyya and A. R. Das, *Tetrahedron Lett.*, 2011, **52**, 4636.
25 C. Yao, S. Lei, C. Wang, T. Li, C. Yu, X. Wang and S. Tu, *J. Heterocycl. Chem.*, 2010, **47**, 26.
26 V. N. Mahire, G. P. Patil, A. B. Deore, P. G. Chavan, H. D. Jirimali and P. P. Mahulikar, *Res. Chem. Intermed.*, 2018, **44**, 5801.
27 N. Kaur, K. Kaur, T. Raj, G. Kaur, A. Singh, T. Aree, S.-J. Park, T.-J. Kim, N. Singh and D. O. Jang, *Tetrahedron*, 2015, **71**, 332.
28 B. Sadeghi, M. Bouslik and M. R. Shishehbore, *J. Iran. Chem. Soc.*, 2015, **12**, 1801.
29 P. Chavan, S. Bangale, D. Pansare, R. Shelke, S. Jadhav, S. Tupare, D. Kamble and M. Rai, *J. Heterocycl. Chem.*, 2020, **57**, 3326.
30 B. Ludi and M. Niederberger, *Dalton Trans.*, 2013, **42**, 12554.
31 M. Stoller and J. M. Ochando-Pulido, *Nanomaterials*, 2020, **10**, 1321.
32 J. Safaei-Ghomi and M. A. Ghasemzadeh, *S. Afr. J. Chem.*, 2014, **67**, 27.
33 M. Zabihzadeh, A. Omidi, F. Shirini, H. Tajik and M. S. N. Langarudi, *J. Mol. Struct.*, 2020, **1206**, 127730.
34 G. Nagaraju, S. Prashanth, M. Shastri, K. Yathish, C. Anupama and D. Rangappa, *Mater. Res. Bull.*, 2017, **94**, 54.
35 A. Kołodziejczak-Radzimska, E. Markiewicz and T. Jesionowski, *J. Nanomater.*, 2012, **2012**, 1.
36 H. R. Shaterian, M. Ghashang and M. Feyzi, *Appl. Catal., A*, 2008, **345**, 128.
37 X. Zhao, J. Zhang, L. Shi, M. Xian, C. Dong and S. Shuang, *RSC Adv.*, 2017, **7**, 42159.
38 M. Seddighi, F. Shirini and M. Mamaghani, *C. R. Chim.*, 2015, **18**, 573.
39 M. Bououdina, S. Azzaza, R. Ghomri, M. N. Shaikh, J. Dai, Y. Song, W. Song, W. Cai and M. Ghers, *RSC Adv.*, 2017, **7**, 32931.

40 D. Survase, B. Bandgar and V. Helavi, *Synth. Commun.*, 2017, **47**, 680.
41 W. M. Basyouni, S. Y. Abbas, N. M. Abdelazeem, K. A. El-BayoukiM and Y. El-Kady, *Synth. Commun.*, 2019, **49**, 3112.
42 M. Abedini, F. Shirini, M. Mousapour and O. Goli Jolodar, *Res. Chem. Intermed.*, 2016, **42**, 6221.
43 B. Hemmati, S. Javanshir and Z. Dolatkhah, *RSC Adv.*, 2016, **6**, 50431.
44 F. Shirini, M. Seddighi and O. Goli-Jolodar, *J. Iran. Chem. Soc.*, 2016, **13**, 2013.
45 N. L. Far, E. Rostami and G. R. Bardajee, *Res. Chem. Intermed.*, 2021, **47**, 4721.
46 R. Pourhasan Kisomi, F. Shirini and M. Golshekan, *Appl. Organomet. Chem.*, 2021, **35**, 6212.
47 A. Bahrani and Z. Karimi-Jaberi, *J. Heterocycl. Chem.*, 2019, **29**, 337.
48 B. Adrom, M. T. Maghsoodlou, N. Hazeri and M. Lashkari, *Res. Chem. Intermed.*, 2015, **41**, 7553.
49 H. Shaterian and M. Mohammadnia, *S. Afr. J. Chem.*, 2013, **66**, 60.
50 A. Shaabani, A. Rahmati, A. H. Rezayan, M. Darvishi, Z. Badri and A. Sarvari, *QSAR Comb. Sci.*, 2007, **26**, 973.
51 M. Mashhadinezhad, F. Shirini, M. Mamaghani and M. Rassa, *Polycyclic Aromat. Compd.*, 2019, **38**, 1417.
52 Y. Mardani, Z. Karimi-Jaberi and M. J. S. Fard, *Z. Naturforsch., B: J. Chem. Sci.*, 2021, **76**, 385.
53 S. Rostami, S. N. Azizi and F. Rigi, *Iran. J. Catal.*, 2017, **7**, 267.
54 O. Goli-Jolodar and F. Shirini, *J. Iran. Chem. Soc.*, 2016, **13**, 1077.